Advances in Bioscience and Bioengineering
2024; 12(1): 1-13
http://www.sciencepublishinggroup.com/j/abb
doi: 10.11648/abb.20241201.11
ISSN: 2330-4154 (Print); ISSN: 2330-4162 (Online)

CO_2 Control Strategy for Large-Scale Cell Culture Bioreactor Operation

Naveenganesh Muralidharan*, Thatsinee Johnson, Emma Bolduc, Mark Davis

Manufacturing Science and Technology (MSAT), AGC Biologics, Boulder, USA

Email address:

nmural@agcbio.com (Naveenganesh Muralidharan)

*Corresponding author

To cite this article:

Naveenganesh Muralidharan, Thatsinee Johnson, Emma Bolduc, Mark Davis. (2024). CO_2 Control Strategy for Large-Scale Cell Culture Bioreactor Operation. *Advances in Bioscience and Bioengineering*, *12*(1), 1-13. https://doi.org/10.11648/abb.20241201.11

Received: January 3, 2024; **Accepted**: January 17, 2024; **Published**: February 1, 2024

Abstract: In most mammalian cell culture operations, the pH is targeted to be close to neutral and the dissolved carbon dioxide [dCO_2] concentration is desired to remain between 5 and 15% to avoid any inhibitory effects on cell growth. Typical cell culture scale-up approaches include maintaining constant power by volume (P/V) or a constant tip speed to set the impeller agitation rate or constant vvm to set the gas flow rate. However, these approaches are only focused on keeping the shear in the bioreactor system to a minimum and do not account for controlling the [dCO_2] concentration within the desired range. Process engineers across industries have remediated the elevated [dCO_2] concentration problem in large scale bioreactors by increasing gas flow rates; however, this approach is often trial and error. Therefore, in this article we review the current understanding of various factors that impact the dCO_2 concentration during the scale up of the cell culture process to large-scale bioreactors. This article also describes an easy and practical approach to predict and control the dCO_2 concentration in large-scale cell culture bioreactors using a mathematical predictive model developed based on mass-transfer first principles. We demonstrate the effective application and verification of the model by running a CHO cell culture process with a peak cell density of up to 20 $x10^6$ Cells/mL in a 15,000 L bioreactor working volume.

Keywords: Bioreactor Scale Up, CO_2 Control, Kla, Cell Culture CO_2 Concentration, CO_2 Predictive Model, CO_2 Bubble Saturation Time

1. Introduction

Elevated CO_2 concentrations have adverse impacts on cell health, causing changes in metabolic state, decreased cell productivity, and altering the glycosylation profile of therapeutic proteins [1]. Inhibitory effects on cell growth and productivity start at CO_2 concentrations 15% that of atmospheric pressure (760 mmHg), i. e., 115 mmHg [1]. Therefore, in biologics production, the CO_2 concentration in a cell culture bioreactor must be maintained below 115 mmHg. However, during scale up of bioreactor operations, maintaining the CO_2 profile below this maximum limit is considered challenging.

The simplest methodology that is most frequently used by process engineers to control CO_2 concentrations is manual feedback control. In this method, the dissolved CO_2 level in the cell culture liquid is measured, and if it exceeds a threshold value (i.e., the action limit), the overall gas flow rate is increased by a certain amount [2]. However, a problem in manual feedback CO_2 control is identifying the correct increment for the total gas flow rate. This increment is often determined by trial-and-error, exposing the process to the risk of uncertainty. Accordingly, in the present study, we derived a sound mathematical model to predict and control the dissolved CO_2 concentration in a cell culture bioreactor as function of KLa, pH set point, viable cell density, lactate, and the bicarbonate profile of the culture. The models have been verified in 15,000L bioreactor scale. This simplified model should help readers to predict and control CO_2 profiles in manufacturing-scale bioreactors easily. Furthermore, we discuss the current state of understanding on factors impacting excessive dissolved CO_2 accumulation in large-scale bioreactors in terms of geometrical bioreactor design and sparger configuration.

2. Impact of Excessive CO_2 Concentration to Cell Culture Performance

For a typical fed-batch cell culture, CO_2 is produced by cellular respiration as cells metabolize glucose, which plays a major role in energy production to support cell growth rate and productivity. Transport of polar and charged molecules like sugars and ions occurs through restrictive selective process in lipid bilayer membranes of the cells. However, uncharged molecules like CO_2 can freely diffuse through the lipid bilayer membrane. When excessive CO_2 enters the cytoplasm, it reacts with water to produce hydrogen ions, which changes the intracellular pH. This causes cells to spend energy on maintaining the pH rather than cell growth and protein expression, as shown in Figure 1. In mammalian cell culture operation, cells consume glucose and produce lactate during exponential growth phase, later when the cells approach stationary phase cell switch the carbon consumption source from glucose to lactate, this metabolic switch in carbon source is defined Lactate metabolic shift (LMF). This LMF is desired in cell culture operation as it drives the process towards high titer yields and better quality on the protein. However, elevated CO_2 levels have been shown to delay or sometime inhibit the cells from undergoing desired lactate shift causing lactate accumulation in culture broth resulting in drop in pH leading to more base titrant addition by bioreactor's pH control. Increase in base titrant addition increases the osmolality, leading to inhibition of cell growth, thereby poor productivity, and variability in glycosylation profile in the therapeutic protein produced [3-6].

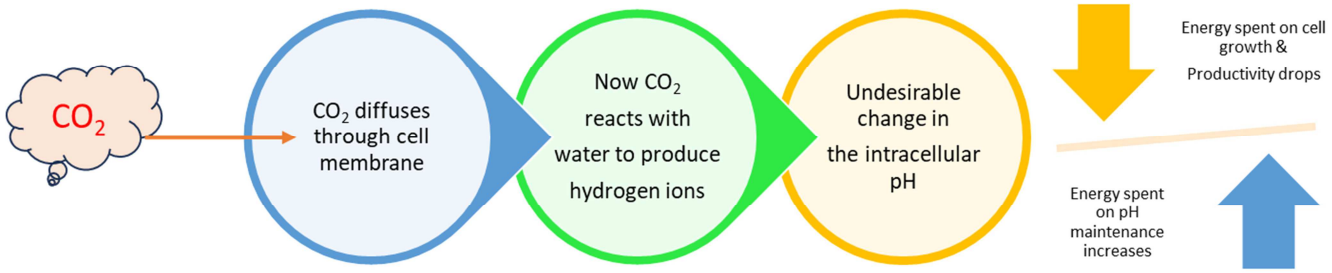

Figure 1. *Impact of excessive CO_2 concentration on cell culture performance.*

3. Factors Impacting Excessive CO_2 Accumulation

3.1. Effect of CO_2 Mass Transfer Coefficient

Early in the culture, it is necessary to sparge CO_2 to maintain the pH. However, as the cell density increases in the bioreactor, accumulation of CO_2 occurs due to cellular respiration. For a typical cell culture process, for every mole of oxygen consumed, one mole of CO_2 is produced (Respiratory Quotient [RQ] = 1) [7]. Therefore, to maintain an optimal CO_2 concentration inside a bioreactor, oxygen transfer and CO_2 removal should be balanced. In other words, the O_2 transfer rate should be equal to the CO_2 transfer rate, as expressed in (1).

$$OTR = CTR \Rightarrow KLa_{O2}\left(C^*_{BO2} - C_{L,O2}\right) = -KLa_{CO2}\left(C^*_{B,CO2} - C_{L,CO2}\right) \quad (1)$$

Here, KLa is the volumetric oxygen transfer coefficient, C_B* and C_L are the molar concentrations of O_2 or CO_2 in the purged gas bubble and liquid, respectively.

KLa is the product of KL (the film transfer coefficient) and a, i.e., the interfacial surface area per volume of the culture (m^2/m^3). Both CO_2 and O_2 experience the same interfacial surface area and hydrodynamic conditions inside the bioreactor, but KL differs for CO_2 and O_2, and it is proportional to the liquid phase diffusivity of the respective gases, as shown in (2).

$$K_L = \sqrt{\frac{4.D_L.\vartheta_B}{\pi.d_B}} \quad (2)$$

Here, D_L is the diffusivity, ϑ_B is the bubble velocity, and d_b is the bubble diameter. The diffusion constants for O_2 and CO_2 at 37°C are calculated as 3.4×10^{-9} and 2.9×10^{-9} m^2/s, respectively, using Wilke and Chang's (1955) method, as shown in (3) [8].

$$D_L = \frac{1.173\times10^{-13}\times(A_{ss}.M)^{0.5}.T}{\mu\times V_m^{0.6}} \quad (3)$$

Applying the diffusivities of CO_2 and O_2 in (2), the mass transfer coefficient ratio of CO_2 to O_2 (Φ) is 0.90. This is in alignment with previously reported Φ values for large bubbles under laminar flow equal to 0. 90. [9, 20].

Φ values below 0.90 have also been reported for micro spargers and at aggressively high gas flow rates using drilled hole spargers. The gas flow conditions for laminar flow can be assessed based on the bubble Reynolds number satisfying the condition of being less than 2000 (bubble Reynolds number is calculated per (8)) [10]. Reduced Φ values far below 0.90 at aggressive turbulent gas flow rates or while using micro spargers will reduce the CO_2 Kla in comparison to O_2 Kla and thereby increase excessive CO_2 accumulation. For gas flow rates to support up to 20×10^6 cells/mL in our 15,000-L

bioreactor operating volume with sparger configuration (28 × 1.6 mm hole diameter), we satisfy the condition for laminar flow (i.e. Bubble Reynolds number < 2000). Therefore, the assumption of Φ = 0.90 is valid for our bioreactor operating conditions. Readers must carefully evaluate their sparger configuration and bubble Reynolds number using (18) before assuming Φ value of 0.90. It is also recommended to perform a separate Kla study specifically for CO_2 when gas flow rate Reynolds numbers is > 2000 and does not satisfy the conditions for laminar gas flow.

3.2. Effect of CO_2 Bubble Saturation Time

The changes in the concentrations of CO_2 and O_2 inside a gas bubble that is rising in a liquid column can be expressed as shown in (4) and (5) [12].

For changes in O_2 concentration in a bubble:

$$\frac{dC_{O2}}{dt} = m_{O2}.K_{G,O2} \times \left(\frac{A_b}{V_b}\right) \times \left(C_{b,O2} - {C_{L,O2}}^*\right) \quad (4)$$

Here,

$$m_{O2} = H_{O2}.R.T$$

$$m_{O2} = H_{O2}.R.T;\ K_{G,O2} = \left(\frac{D_{O2}}{\delta}\right)\ ;\ V_b = \frac{4}{3}\pi {r_b}^3;$$

$$A_b = 4\pi {r_b}^2$$

$$\frac{dC_{CO2}}{dt} = m_{O2}.K_{G,CO2} \times \left(\frac{A_b}{V_b}\right) \times \left({C_{L,CO2}}^* - C_{b,CO2}\right) \quad (5)$$

Here,

$$m_{CO2} = H_{CO2}.R.T;\ K_{G,CO2} = \left(\frac{D_{CO2}}{\delta}\right)$$

Here; $K_{G,O2}$ and $K_{G,CO2}$ are the overall gas phase mass transfer coefficients for O_2 and CO_2 respectively, D_{O2} and D_{CO2} are the diffusion coefficients for O_2 and CO_2, respectively, δ is the thickness of the bubble film (δ = 50 μm is a good approximation [17]), A_b is the surface area of a single bubble in m^2, V_b is the volume of a single bubble in m^3, C_B stands for the O_2 or CO_2 concentration of a bulk gas-phase bubble expressed in mmHg, C_L is the liquid phase concentration that is in equilibrium with the gas phase. m is defined as the partition constant. "m" is the function of the solubility of a gas. CO_2 and O_2 have different solubilities in a fluid, as given by Henry's coefficient expressed as the amount of gas that is solubilized per unit volume of the liquid per unit pressure in mmol/L.atm. The values of Henry's coefficient (H) are 25×10^{-3} and 1×10^{-3} mol/L.atm for CO_2 and O_2, respectively. Therefore, CO_2 is 25 times more soluble in liquid than oxygen in atmospheric pressure.

For illustration, assume a 0.5-mm-diameter air bubble is rising in a liquid, and the size of the bubble remains constant with no shrinkage throughout its lifetime. Assuming air is purged through the sparger at atmospheric pressure (760 mmHg) and the mole faction of O_2 in air is 0.21, then the O_2 concentration in the sparged air bubble is 159 mmHg (0.21 × 760 mmHg). For dissolved oxygen (DO), the set point of 40% is equal to 64 mmHg (0.40 × 0.21 × 760 mmHg). Then the O_2 and CO_2 concentrations in the bubble at time zero are 159 and 0 mmHg, respectively, and the liquid O_2 and CO_2 concentrations are 64 and 115 mmHg, respectively. A sample calculation for changes in the O_2 and CO_2 concentrations in the bubble using (4) and (5) is shown in Figure 2A and 2B. Figure 2C shows the change in the concentration of O_2 and CO_2 in the bubble, demonstrating that the bubble attains 95% saturation for CO_2 between 5 to 6 s. This value is in alignment with previously reported experimental values of between 5 and 9 s [3, 13]. Therefore, the driving force for CO_2 drops to zero after 6 s and no further CO_2 can be transferred into the bubble. On the other hand, for O_2 transfer, bubble O_2 concentration falls relatively slowly, and the bubble continues to supply O_2 to the liquid as it rises. In comparison to O_2, as the bubble attains CO_2 saturation in a short period, it is effective for CO_2 removal only for a small portion of its lifetime. Figure 2D shows that rate of CO_2 bubble saturation can be decreased by increasing the bubble diameter to improve CO_2 removal rate.

3.3. Effect of Bioreactor Liquid Hydrostatic Pressure

Bioreactor aspect ratio, defined as liquid height to tank diameter (H_L/D_T), is typically maintained between 1.0 to 1.5 [14, 15]. While scaling up the operational volume of the bioreactor, the liquid height increases per (6) and thereby increases the hydrostatic pressure P per (7). Fuller et al. (1966) developed an empirical correlation for diffusivity coefficient that shows an inverse relationship to pressure, as shown in (8) [16], (6) to (8) shows as bioreactor height increases thereby total pressure increases and diffusion coefficient deceases; making CO_2 removal from a culture more challenging.

$$V_T = \frac{\pi \times {D_T}^2}{4} \times H_L;\ Rearranging, H_L = \left(\frac{4 \times V_T}{\pi \times 1.5^2}\right)^{1/3} \quad (6)$$

$$P_l = 1\ atm + \left[\rho_L \times g \times H_L \times \frac{(9.87e{-}6\ )atm}{1\ pascal}\right] \quad (7)$$

Diffusivity as a function of pressure and temperature.

$$D_{A,B} = \frac{1.013 \times 10^{-7}.T^{1.75}\left(\frac{1}{M_A} + \frac{1}{M_B}\right)^{1/2}}{P\left[{v_A}^{1/3} + {v_B}^{1/3}\right]^2} \quad (8)$$

Figure 3 shows the increase in the liquid height and corresponding solubility of CO_2 for different bioreactor volumes with an assumed aspect ratio of 1.5.

	A	B	C	D	E	F	G
1	Change in the concentration of CO_2 in gas bubble				Change in the concentration of O_2 in gas bubble		
2	Diffusion coefficient, D, [m^2/s]	2.87E-09			Diffusion coefficient, D, [m^2/s]	3.40E-09	
3	Bubble diameter (mm)	0.5			Bubble diameter (mm)	0.5	
7	Bubble area , A_b (m^2)	7.85E-07			Bubble area , A_b (m^2)	7.85E-07	
8	Bubble volume, V_b (m^3)	6.54E-11			Bubble volume, V_b (m^3)	6.54E-11	
9	Bubble film thickness, δ (m)	5.00E-05			Bubble film thickness, δ (m)	5.00E-05	
10	K_L.(m/S) = D/δ	5.74E-05			K_L.(m/S) = D/δ	6.80E-05	
11	H, mol/L.Atm	2.50E-02			H, mol/L.Atm	1.07E-03	
12	Partition constant, m	0.64			Partition constant, m	0.03	
13	K_G. (A_b/V_b), (1/s)	4.38E-01			K_G. (A_b/V_b), (1/s)	2.22E-02	
14	Liquid dissolved CO_2 Conc; C_L (mmHg)	115			Liquid dissolved O_2 Conc; C_L (mmHg)	64	
15	Time (s)	ΔC = K_G. (A_b/V_b).(C_L - C_b)	$C_b = \Delta C_{n-1} + C_{b\,(n-1)}$		Time (s)	ΔC = K_G. (A_b/V_b).(C_b - C_L)	$C_b = C_{b\,(n-1)} - \Delta C_{n-1}$
16	0	50.4	0		0	2.1	159
17	1	28.3	50.4		1	2.1	156.9
18	2	15.9	78.7		2	2.0	154.8
19	3	8.9	94.6		3	2.0	152.8
20	4	5.0	103.6		4	1.9	150.8
21	5	2.8	108.6		5	1.9	148.9

2A: Change in the concentration of O_2 in gas bubble calculation

2B: Change in the concentration of CO_2 in gas bubble calculation

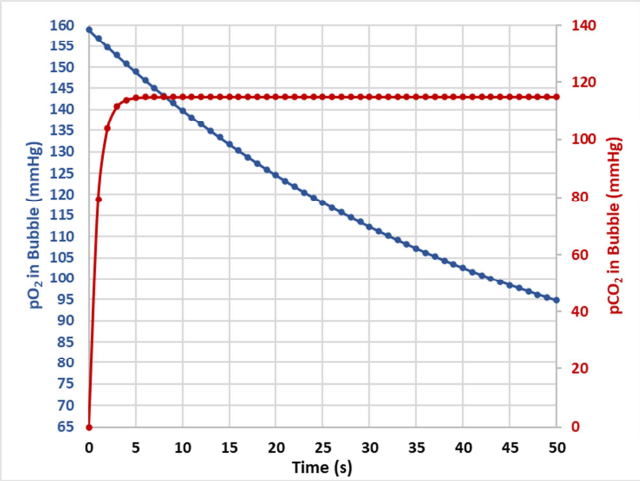

2C: Bubble Saturation time for CO_2 and O_2 in a bubble with 0.5 mm diamter

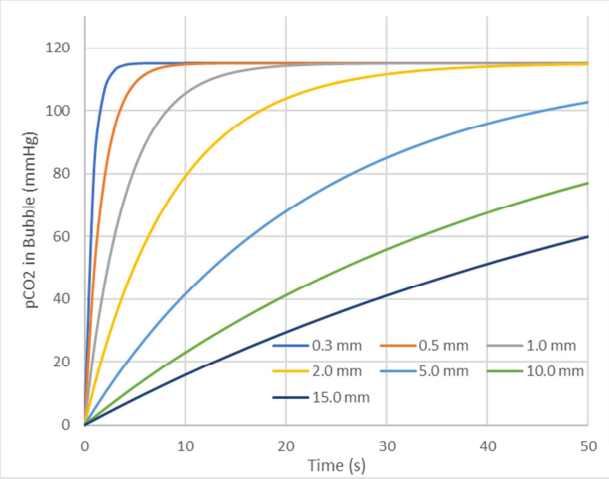

2D: Bubble Saturation time for CO_2 for different bubble diamters

Figure 2. *Bubble saturation time.*

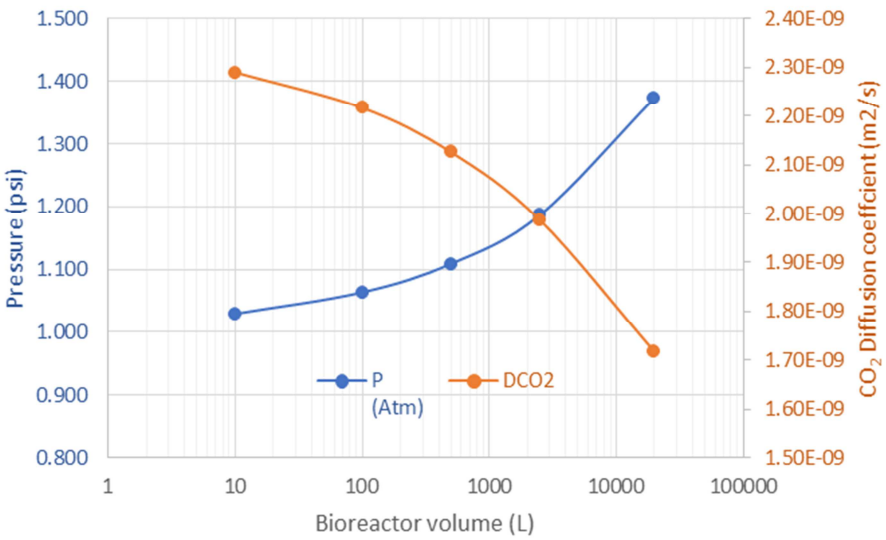

Figure 3. *Impact of bioreactor height.*

3.4. Effect of Difference in O_2 and CO_2 Driving Force

As the bubble germinates and rises through the liquid, the period of time from bubble generation to the bubble reaching the gas–liquid surface and disappearing is defined as bubble residence time ($T_{B,R}$). During its lifetime in the liquid, a bubble serves two purposes for cell culture operation: 1) transferring O_2 from the bubble into the liquid, and 2) removing dissolved CO_2 from the liquid to the bubble. The rate of both O2 transfer and CO_2 removal depends on driving force, $\Delta C = C_s - C_T$. Here, C_S and C_T are the starting and target concentrations of the gas species in the bubble. ΔC dictates the driving force of gas mass transfer. For O_2 transfer: Assuming air is purged through the sparger at atmospheric, the O_2 concentration in the sparged air bubble $C_{S,O2}$ is 159 mmHg (0.21 × 760 mmHg).% DO set point ($C_{T,O2}$) of 40% is equal to 64 mmHg (0.40 × 0.21 × 760 mmHg). The driving force for O_2 transfer is calculated to be 96 mmHg, as shown in (9) [1].

$$\Delta C_{O2} = \left(C_{s,O2} - C_{T,O2}\right) = 96\ mmHg \tag{9}$$

For CO_2 transfer: The driving force for the CO_2 is expressed in (10).

$$\Delta C_{CO2} = \left(C_{T,CO2} - C_{Equil,CO2}\right) \tag{10}$$

Here, $C_{T,CO2}$ is the desired maximum pCO_2 limit (115 mmHg) and $C_{Equl,CO2}$ is dissolved CO_2 concentration in equilibrium with the gas stream. To remove CO_2 from the liquid at the same rate as the transfer of O_2 to the liquid, we need driving force ΔCO_2 equal to ΔO_2. Hence equating (9) and (10) and solving for $C_{Equl,CO2}$ will yield a value of 19 mmHg, as expressed in (11).

$$C_{Equil,O2} = (115 - 96)\ mmHg = 19\ mmHg \tag{11}$$

This value of 19 mmHg is only 2.5% of atmospheric pressure (760 mmHg). This means, as the bubble rises, when the CO_2 concentration in the bubble reaches 19 mmHg, the CO_2 removal rate drops below the O_2 transfer rate. Therefore, we define 19 mmHg as the rate-limiting maximum bubble CO_2 concentration, [$C_{CO2,RL}$], and time for the bubble to reach the maximum rate-limiting CO_2 concentration is defined as the bubble CO_2 rate-limiting equilibrium time $T_{B,RL}$. If the bubble residence time T_{BR} is less than $T_{B,RL}$, then the bubble is efficient in removing CO_2 throughout its lifetime. If T_{BR} is larger than $T_{B,RL}$, then the bubble is efficient in CO_2 removal equivalent to O_2 transfer only until time $T_{B,RL}$. Hence, larger fast rising bubbles with shorter residence times are more efficient than smaller bubbles with longer residence times [1, 7].

For a typical cell culture bioreactor process, O_2 KLa is enhanced by using micro spargers and/or a blend of pure O_2 and air to increase the driving force ΔC. Both lead to sufficient O_2 transfer rates using low gas flow rates, which further enhances the accumulation of CO_2 at the large scale.

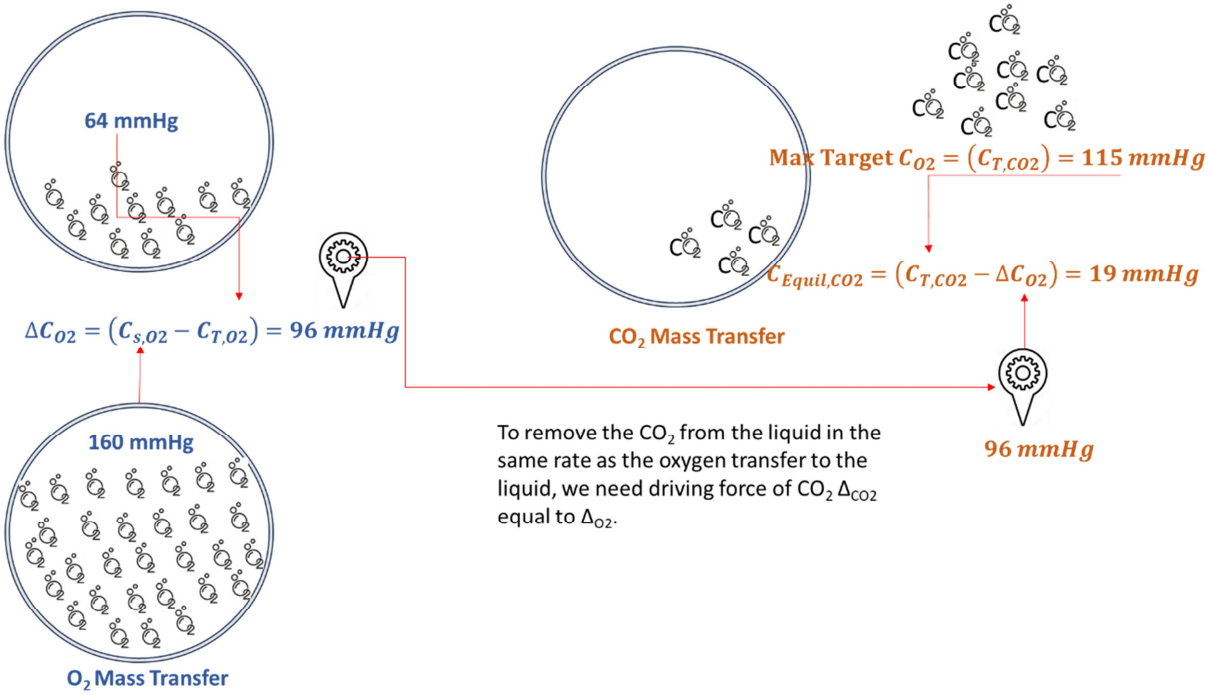

Figure 4. *Difference in O_2 and CO_2 driving forces on excessive CO_2 accumulation.*

3.5. Effect of Sparger Design and Gas Entrance Velocity

As discussed before, bubble residence time plays a critical role in the dissolved CO_2 concentration in a culture broth. The faster the bubble travels through the liquid column, the more efficient is the CO_2 transfer rate. The bubble velocity is a function of bubble size. The bubble size and bubble velocity can be calculated using (12) to (17) [17, 18].

$$GEV = \frac{Q_g}{n_O\left(\frac{\pi d_O^2}{4}\right)} \quad (12)$$

$$d_b = 1.17.GEV^{0.4}.d_O^{0.8}.g^{0.2} \quad (13)$$

$$V_1 = \frac{1}{36} \times \frac{\left(\rho_L - \rho_g\right).g.d_b^2}{\mu_L} \quad (14)$$

$$V_2 = V_1\left[1 + 0.73667\,\frac{(g.d_b)^{1/2}}{V_1}\right]^{1/2} \quad (15)$$

$$V_3 = \left(\frac{3.\sigma}{\rho_L.d_b} + \frac{g.d_b.(\rho_L - \rho_g)}{2.\rho_L}\right)^{1/2} \quad (16)$$

$$\vartheta_b = 1 \div \sqrt{\frac{1}{{V_2}^2} + \frac{1}{{V_3}^2}} \quad (17)$$

$$N_{Bubble,Re} = \frac{d_O.GEV.\rho}{\mu} \quad (18)$$

Figure 5 shows the bubble rise velocity as a function of bubble diameter. Bubbles with sizes less than 0.1 mm (or 100 µm), called microbubbles, have low rising velocities. Here, the bubble movement is dominated by liquid surface tension leading to reduced bubble rising velocity, causing longer bubble residency time in the bioreactor and poor CO_2 removal from the cell culture. Smaller bubbles give higher mass transfer areas, but also have slow rising velocities and reduced CO_2 driving force. Therefore, the optimum operating conditions for effective CO_2 removal is a sparger flow rate that maintains the ratio of bubble residence time to bubble saturation time ≥ 1.0.

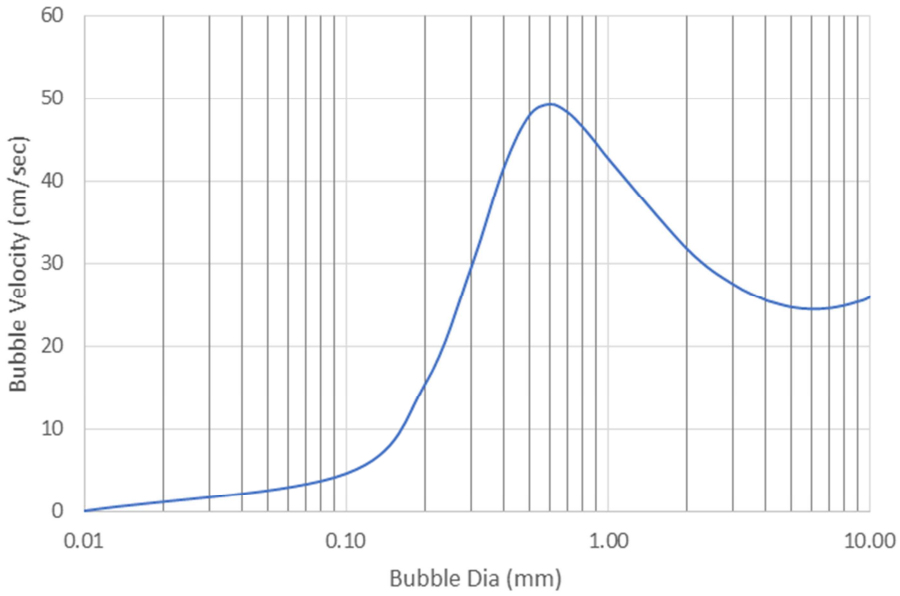

Figure 5. *Bubble diameter vs. bubble rise velocity.*

4. CO_2 Predictive Model Assumptions and Limitations

4.1. Assumptions

1. The rate of mass transfer is much faster than the O_2 uptake rate and CO_2 evolution rate of cells. Therefore, the mass balance governing equations; O_2 transfer rate equals O_2 uptake rate, and CO_2 transfer rate equals CO_2 evolution rate.
2. The bioreactor mass transfer system is assumed to be at a pseudo-steady state. This means over the very short period of bubble residence time in the bioreactor, the O_2 and CO_2 concentration in the liquid is not changing while the CO_2 concentration in bubbles is dynamic and changing continuously.
3. The cell culture performance attributes, like viable cell density, oxygen uptake rate, lactate profile, and bicarbonate profile, are known from previous at-scale or small-scale runs.
4. This model also assumes the biological metabolite consumption and production rate of cells is conserved across different scales of bioreactor operation and from batch to batch.
5. The sparge rate is sufficiently low to prevent bubble coalescence.
6. As the bubbles rise through the liquid, the drop in O_2 mole fraction from the bubbles is compensated by increase in CO_2 mole fraction in the bubbles.

4.2. Limitations

1. This model can only be used when the bioreactor mass transfer co-efficient (*Kla*) is characterized.
2. The model assumes that the *Kla* from surface gas–liquid interface is small and insignificant compared to the mass transfer from sparging gas bubbles, and is therefore applicable only for large manufacturing-scale bioreactors.
3. The assumption that CO_2 *KLa* = 0.90 times O_2 *KLa* is

applicable only for bubbles generated under laminar conditions using drilled hole spargers and does not apply to bubbles generated using micro spargers or when gas flow rates using drilled hole spargers are operated under turbulent conditions.

4. This model only accounts for major metabolites like CO_2, lactate, and bicarbonate for pH control that are most frequently measured in cell culture process. Therefore, it does not include other organic acids or base components produced by cells during fermentation.

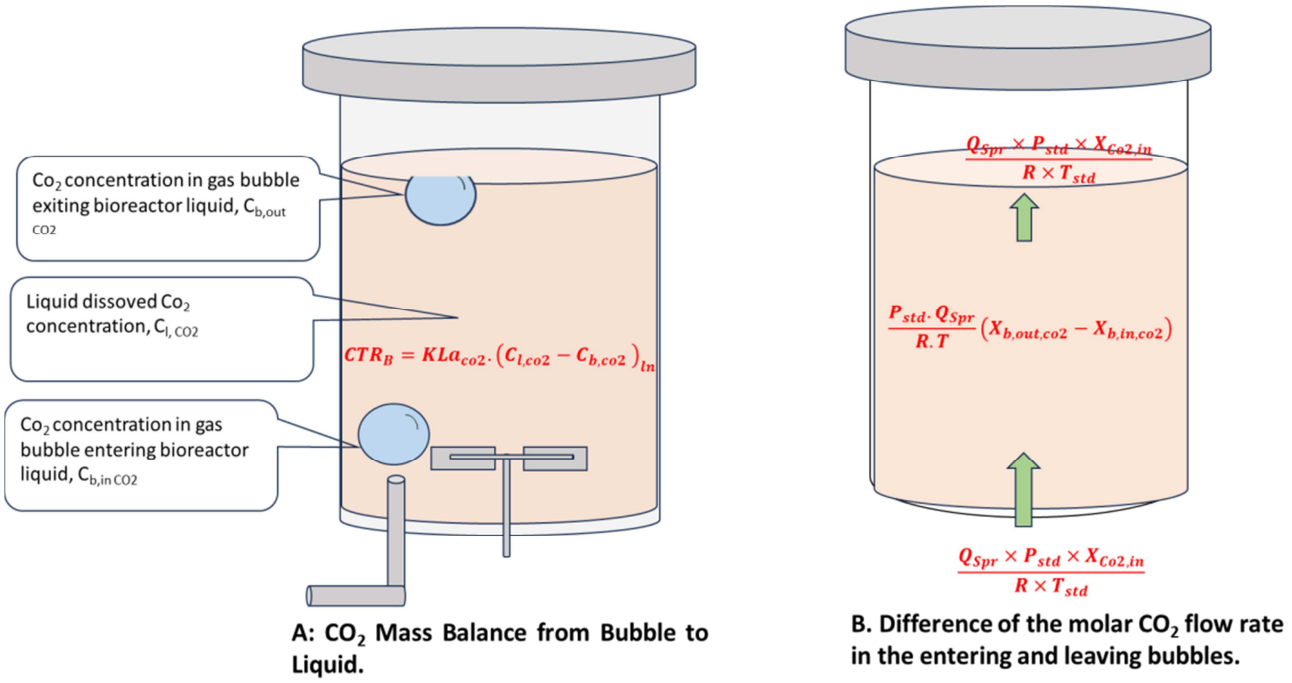

Figure 6. *CO_2 Mass balance for the gas transfer in bioreactor system.*

4.3. CO_2 Predictive Model Development

As shown in Figure 6A, the CO_2 transfer rate from the liquid to sparged gas bubbles can be expressed as shown in (19). Here $C_{,b,CO2}$ represents the CO_2 concentration in the bubble (mmol/L), $C_{l,CO2}$ represents the liquid dissolved CO_2 concentration (mmol/L), and KLa_{CO2} represents the CO_2 mass transfer coefficient (1/h). The suffix (ln) indicates logarithmic mean for driving force. In large-scale bioreactors, because of the gradient of increasing hydrostatic pressure from the surface of the liquid to the bottom of the vessel, the composition of a gas phase bubble is dynamic. Accordingly, the driving force is expressed as logarithmic mean driving force [11].

$$CTR_B.V = KLa_{co2}.V.(C_{l,co2} - C_{b,co2})_{ln} \quad (19)$$

The logarithmic mean gas bubble CO_2 concentration can be expressed as the function of bubble CO_2 concentration entering and leaving the culture liquid in the bioreactor, as shown in (20) [11]. Here, the suffixes $b_{,in,CO2}$ and $b_{,out,CO2}$ indicate CO_2 concentration in bubble going into the liquid and exiting the liquid, respectively.

$$(C_{l,co2} - C_{b,co2})_{ln} = \frac{(C_{b,in,co2} - C_{b,out,co2})}{ln\left(\frac{C_{l,co2} - C_{b,in,co2}}{C_{l,co2} - C_{b,out,co2}}\right)} \quad (20)$$

Substituting (20) in (19) gives (21):

$$CTR_B.V = KLa_{b,co2}\left(\frac{(C_{b,in,co2} - C_{b,out,co2})}{ln\left(\frac{C_{l,co2} - C_{b,in,co2}}{C_{l,co2} - C_{b,out,co2}}\right)}\right).V \quad (21)$$

The dissolved CO_2 concentration in equilibrium with the gas stream in (21) can be expressed as a function of Henry's constant, system pressure, and mole fraction of CO_2, (Concentration, C = P.H.X) by applying Henry's law, as shown in (22) [11]. Here, P_l is pressure (atm), H is the henry coefficient (mol/L.atm), and X is the mole fraction of gas. Suffixes $b_{,in,CO2}$ and $b_{,out,CO2}$ represent CO_2 concentration in a bubble going into the liquid and exiting the liquid, respectively.

$$CTR_B.V = KLa_{b,co2}.V\left(\frac{(X_{b,out,co2}.P_{l,co2}.H_{co2} - X_{b,in,co2}.P_{l,co2}.H_{co2})}{ln\left(\frac{C_{l,co2} - C_{b,in,co2}}{C_{l,co2} - C_{b,out,co2}}\right)}\right) \quad (22)$$

As shown in Figure 6B, the moles of CO_2 transferred from the sparge stream can also be determined from the difference of the molar CO_2 flow rate in the entering and leaving bubbles. If we assume that the gas hold-up volume is constant, then the

CO_2 transfer rate from the sparger can be expressed as shown in (23). Here P_{std} is the standard pressure (Atm), Q_{spr} represents sparger flow rate, R is the relative gas constant, and T is the temperature in K.

$$CTR_B.V = \frac{P_{std}.Q_{Spr}}{R.T}\left(X_{b,out,co2} - X_{b,in,co2}\right) \quad (23)$$

Now equating (22) and (23), will yield (24)

$$KLa_{b,co2}.V\left(\frac{(X_{b,out,co2}-X_{b,in,co2})p_l.H_{co2}}{ln\left(\frac{C_{l,co2}-C_{b,in,co2}}{C_{l,co2}-C_{b,out,co2}}\right)}\right) = \frac{P_{std}.Q_{Spr}}{R.T}(X_{b,out,co2} - X_{b,in,co2}) \quad (24)$$

Simplification of (24) will yield (25).

$$ln\left(\frac{C_{l,co2}-C_{b,in,co2}}{C_{l,co2}-C_{b,out,co2}}\right) = \frac{KLa_{b,co2}.V.R.T.P_l.H_{Co2}}{P_{std}.Q_{Spr}} \quad (25)$$

For simplification in further calculation, the right-hand side of (25) is termed as a constant named A_{CO2}, as this term has no unit all together.

$$\frac{KLa_{b,co2}.V.R.T.P_l.H_{Co2}}{P_{std}.Q_{Spr}} = A_{co2} \quad (26)$$

Substituting (25) in (26)

$$\left(\frac{C_{l,co2}-C_{b,in,co2}}{C_{l,co2}-C_{b,out,co2}}\right) = Exp\,(A_{co2}) \quad (27)$$

Re-arranging the numerator and denominator in (27), the right-hand side of the (27) Exp (A_{CO2}) takes a negative sign as shown in (28).

$$\left(\frac{C_{l,co2}-C_{b,out,co2}}{C_{l,co2}-C_{b,in,co2}}\right) = Exp\,(-A_{co2}) \quad (28)$$

Expressing dissolved CO_2 concentration in equilibrium with the gas stream in (28), as a function of Henry's constant, system pressure and mole fraction of CO_2, (Concentration, C= P. H. X) by the Applying Henry's law will yield (29). [6, 8].

$$\left(\frac{C_{l,co2}-X_{b,out,CO2}.P_l.H_{Co2}}{C_{l,co2}-X_{b,in,CO2}.P_l.H_{Co2}}\right) = Exp\,(-A_{co2}) \quad (29)$$

Rearranging (29) and solving for concentration of CO_2 in bubble exiting the liquid is given by (30):

$$X_{b,out,Co2}.P_l.H_{Co2} = C_{l,co2}\left(1 - Exp(-A_{co2})\right) + X_{b,in,Co2}.P_l.H_{Co2}.Exp(-A_{co2}) \quad (30)$$

Now substituting (26) and (30) in (22) and solving for dissolved $C_{l,CO2}$ will yield (31) to predict the liquid dissolved CO_2 concentration. Refer to Appendix A for details of algebraic mathematical simplification.

$$C_{l,co2} = \frac{CTR_T.A_{co2}+KLa_{b,co2}.X_{b,in,co2}.P_l.H_{Co2}.(1-Exp(-A_{co2}))}{KLa_{b,co2}(1-Exp(-A_{co2}))} \quad (31)$$

Often In cell culture bioreactor operation, liquid dissolved CO_2 is measured as partial pressure of CO_2 (pCO_2) in millimetre mercury (mmHg). The CO_2 concentration calculated using Equation 32 is converted to pCO_2 in mmHg using the ideal gas law (P × V = n × R × T). Rearranging the ideal gas expression will yield dissolved pCO_2 as follows: Here, T is temperature expressed in Kelvin.

$$pCO_2 = C_{l,CO2} \times R \times T \quad (32)$$

In (31), there are two unknown terms: CO_2 transfer rate (CTR) and mole fraction of CO_2 ($X_{b,\,inCO2}$). CO_2 transfer rate can be calculated from CO_2 evolution rate (CER), which in turn is dependent on oxygen uptake rate (OUR) of the cells and respiratory quotient (RQ). CER is calculated as shown in (33). Here RQ is defined as the moles of CO_2 released for every mole of O_2 consumed. Hu (2020) reported a RQ value of 1.0 for mammalian cells [7].

$$CTR = CER = RQ.OUR \quad (33)$$

Mole Fraction of CO_2 (X_b, in CO_2) from Medium Chemistry

Typical cell culture media buffering is achieved using a CO_2-bicarbonate based buffer. The pH of the medium is dependent on the fine balance of dissolved carbon dioxide (CO_2) and bicarbonate (HCO_3^-). Often, cell culture carbonate buffered media is operated around neutral pH. CO_2 reacts with water to form carbonic acid, as shown in (34) [19].

$$CO_2 + H_2O \leftrightarrow \left[HCO_3^-\right] + \left[H^+\right] \quad (34)$$

Assuming the amount of dissolved CO_2 in the culture medium is equal to the amount of CO_2 in gas phase at equilibrium and applying the Henderson–Hasselbalch principle, the cell culture medium buffer can be expressed as shown in (35) [19].

$$pH = pKa + \frac{[HCO3]}{[CO_2]} \quad (35)$$

In mammalian cell culture fermentation, one other metabolite lactate plays a critical role in medium buffer chemistry. Lactate is a predominant metabolite produced by cells that brings the pH into the acidic range in bioreactor environments. Lactate has an equilibrium constant pKa of 5.5. Because a typical cell culture is maintained around neutral pH 7.0, one mole of lactate produced by cells will demand one mole of base titrant for neutralization. Due to this neutralization, the culture broth now displaces the acidic component of the buffer in the form of CO_2 gas. So, the effective concentration of base in the culture will be [HCO_3] − [Lactate] [19]. Based on this reaction in the culture, we can now introduce lactate into the Henderson–Hasselbalch equation, and Equation (35) can be rewritten as shown in (36).

$$pH = pKa + \frac{[HCO3]-[Lactate]}{[CO_2]} \quad (36)$$

Gramer et al. (2007) showed an empirical relationship between pH, CO_2, lactate, and bicarbonate concentration, as shown in (37), and verified the application of the model in (37) using actual cell culture runs [19].

$$[Lac] = [HCO3] - 0.88.[CO_2\%]^{0.79}.10^{(pH-6.38)} \quad (37)$$

Here, lactate and bicarbonate concentrations are expressed in mmol/L, CO_2 concentration is expressed in %.

Based on the correlation expression shown in (37), a contour plot was created showing the lactate concentration in g/L as a function of pCO_2 in (%) and bicarbonate concentration in mMol for four different pH values ranging from 6.90 to 7.05 typically used for cell culture, as shown in Figure 7. The mole fraction of CO_2 in the gas purge can be calculated based on the cell culture lactate and bicarbonate concentrations. In some cell culture platform process, post inoculation rather than calling CO_2 under pH control, CO_2 is sparged between 5 to 10% for a specific short period of time between 24 to 48 hours to ensure specific amount of CO_2 is maintained in the culture, in such instances mole fraction sparged CO_2 gas is substituted for the value of $X_{b,in,CO2}$ instead of using Figure 7.

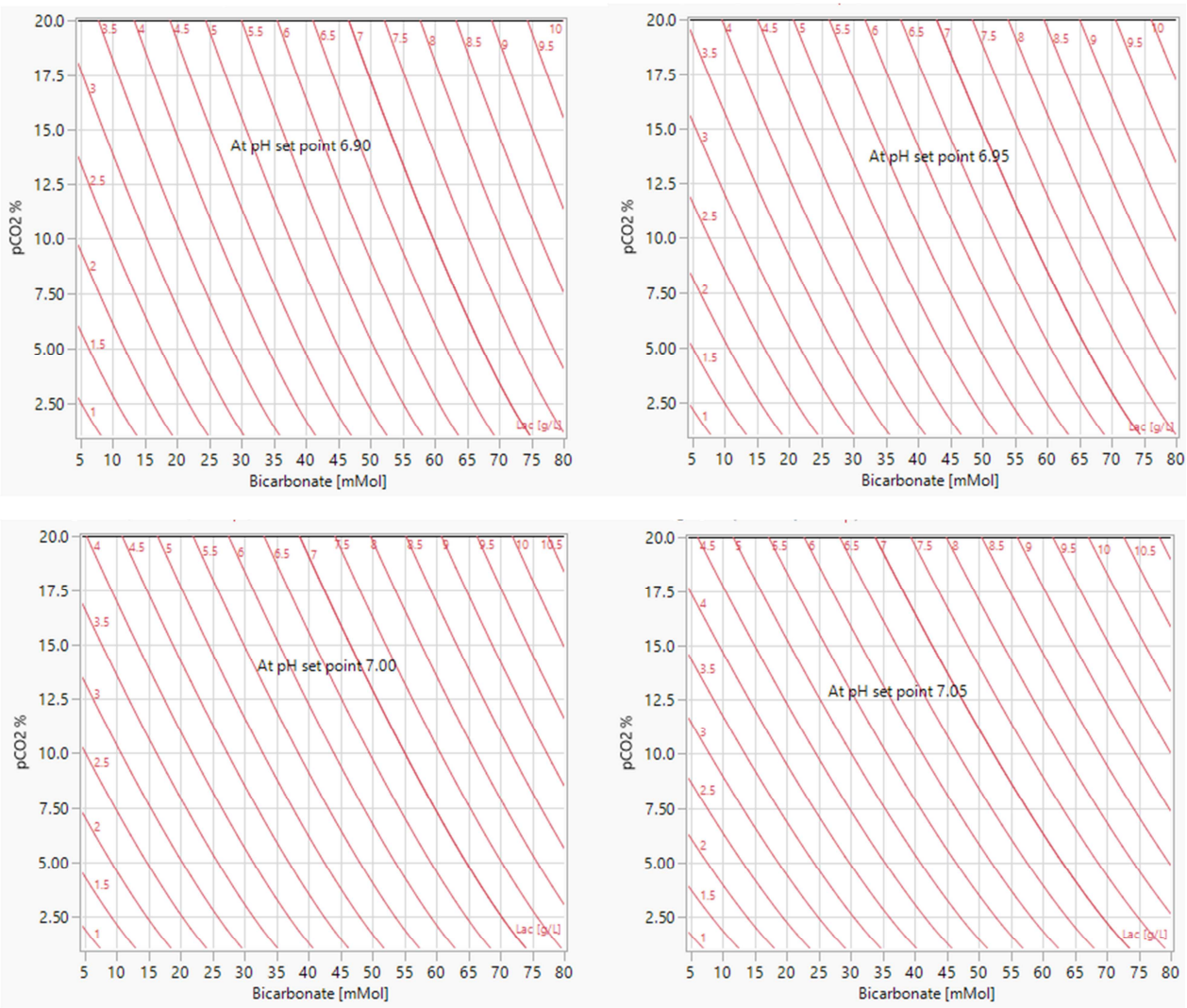

Figure 7. *Correlation between pH, pCO_2, lactate, and bicarbonate to determine the mole fraction of CO_2 ($X_{b,inCO2}$).*

5. At Scale Model Verification and Successful Implication of Predictive Model

We ran a high cell density CHO cell culture process up to 20 × 10^6 cell/mL peak cell density in 15,000L bioreactor working volume. The pCO_2 concentration was measured using Nova Flex 2 metabolite analyzer. Twenty-three actual measured pCO_2 values are plotted against the predicted values as shown in Figure 8A, linear regression of predicted over measured CO_2 values gave an $R^2 = 0.87$ demonstrates, that the predictive expression is reliable. Additionally, the p-value less than 0.001 demonstrates the measure of strength of association between the predicted and actual values is statistically significant. Figure 8B shows Density Ellipse fit. The density ellipse shows the degree of correlation between the predictive and

explanatory variable using correlation coefficient and its p value. The correlation coefficient shown in Figure 8C is the Pearson correlation coefficient (r) and it is the most common way of measuring a linear correlation. It is a number ranging between –1 and 1 that measures the strength and direction of the linear relationship between two variables. r = 0.93 demonstrates, that there is a linear relationship between predicted and actual pCO_2 values is strong and p value of <0.0001 for regression coefficient "r" signifies that the linear relationship is statistically significant. Figure 8C shows the residual plot at different measured actual CO_2 concentration. Figure 8C, demonstrates for 19 out of 23 data points the absolute difference between the measured and predicted CO_2 values are within ± 10 mmHg which is the expected range for QC level-1 standard check with the mean pCO_2 value of 70 mmHg for NovaFlex2 metabolite analyzer. Furthermore, as the measurement range increases, the acceptable expected range also increases that explains the higher residual values at measured pCO_2 above 100 mmHg. NovaFlex2 analyzer used for this study does not have any QC standard checks above 70 mmHg.

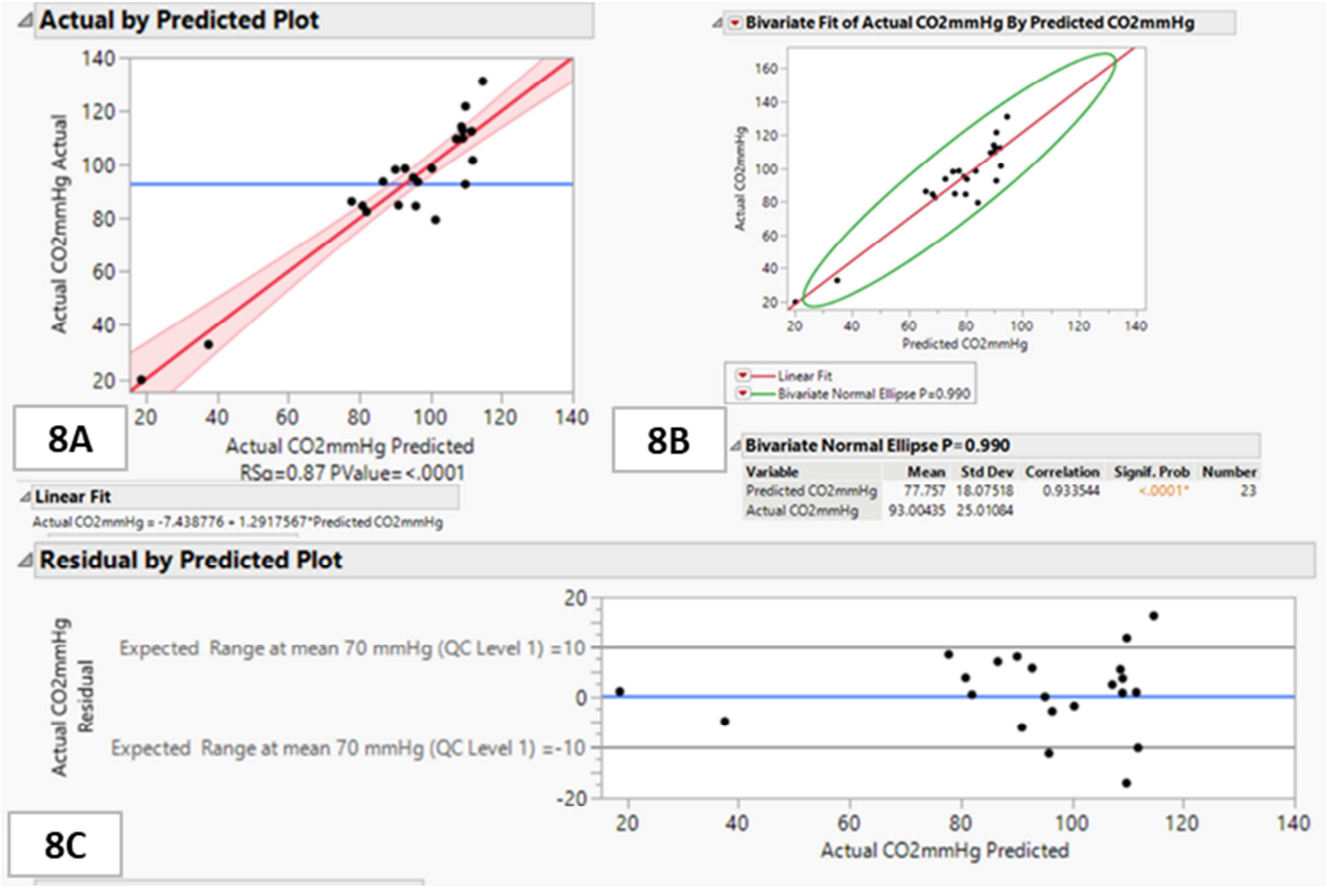

Figure 8. *pCO_2 predictive model validation.*

6. Sample Design Space for Bioreactor Operation to Control pCO_2

A contour plot was drawn to predict the dissolved CO_2 concentration using (31) with sparger total gas flow rate and viable cell density as explanatory variables, as shown in Figure 9. The assumptions for the parameters in the predictive model are summarized in Table 1, based on the values reported by Hu (2022), to represent typical production bioreactor operating conditions [1, 7].

Additionally, Equation (31) demands two more input values, that is CO_2 mole fraction and Kla. For CO_2 mole fraction, Figure 7 is used with the assumptions in Box 1; A CO_2 mole fraction of 5% is calculated. 4 to 7% is a good approximation to cover a wide range of cell culture operation. For KLa value, a predictive expression created by experimental studies is used, as reported in our previous published article Muralidharan et al. (2024) [17]. Based on the above assumptions, a contour profile was created showing pCO_2 profile as a function of gas flow rate and viable cell density, as shown in Figure 9.

Table 1. *pCO_2 Predictive Model Assumptions.*

Henry Coefficient H = 25 mmol/L. Atm
Temperature 37°C
pH set point = 7.00
Bicarbonate concentration = 35 mmol/L
Lactate concentration = 4.0 g/L.
Bioreactor Volume = 15,000 L
Impeller Agitation Rate = 30 RPM

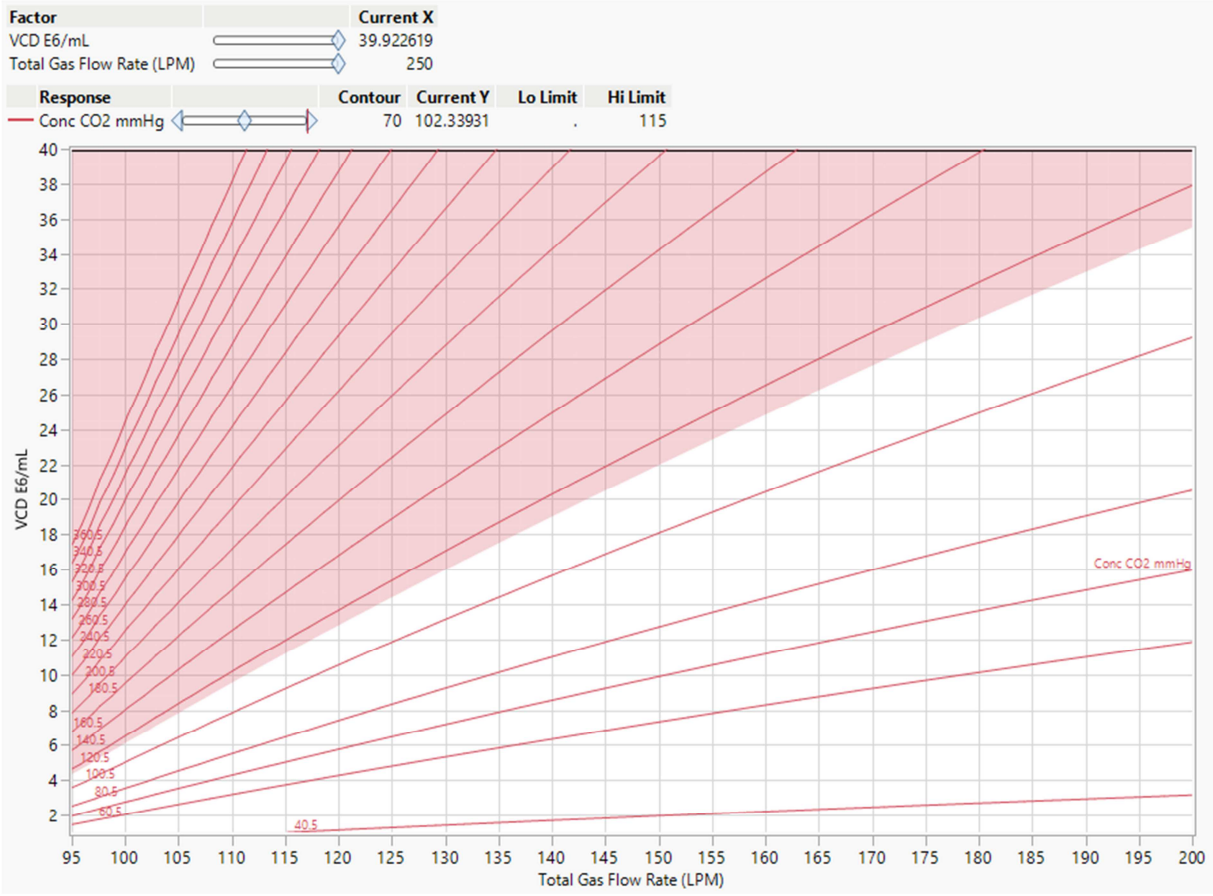

Figure 9. *pCO_2, design space for bioreactor operating conditions.*

7. Conclusions

This article summarizes the impact of excessive CO_2 accumulation in cell culture operation, considering factors in scaling up that cause the CO_2 accumulation. A predictive model to predict and control CO_2 accumulation in large manufacturing-scale bioreactors is presented. Readers are encouraged to carefully weigh the limitations of this model to assess its suitability before applying it to their systems. As shown in Figure 8, there is an offset between the predicted to actual pCO_2 value. This could be due to variability of measurement instrument and the limitations of the assumptions in the model. However, the application of this model is to estimate the increment in total gas flow rate required to control excessive CO_2 accumulation.

Abbreviations

A_{ss}: Association factor for the solvent (-). 2.6 for water.

C: Molar concentrations of gas in purged gas or liquid. (mmol/L or mmHg).

CTR: Corbon dioxide Transfer Rate (mmol/L.hr)

d_B: Bubble diameter (m)

d_o: Sparger hole / orifice diameter (m)

D: Diffusion Coefficient (m^2/s)

D_T: Diameter of the tank (m)

g: Specific gravity 9.8 (m/s^2)

GEV: Gas entrance velocity (m/s)

H_L: Liquid height in the tank (m)

H_{O2} and H_{CO2}: Henry's coefficient (H) is 25×10^{-3} and 1.07×10^{-3} mol/L.atm for CO_2 and O_2, respectively.

K_L: Film transfer coefficient (m/s)

KLa: Overall mass transfer coefficient for O_2 and CO_2 (1/hr).

M, M_A and M_B: Molecular weights of the solute and solvent in g/mol ($M_{CO2} = 44$, $M_{O2} = 32$, $M_{H2O} = 18$).

m_{O2} and m_{CO2}: Partition coefficient is 0.64 and 0.03 (-) for CO_2 and O_2, respectively.

OTR: Oxygen Transfer Rate (mmol/L.hr)

P_l: Total pressure in the system (Atm)

Q_g: Volumetric sparger gas flow rate (m^3/s)

R: Relative gas constant, 8.21E-5 L/Atm/mmol.K

r_b: Bubble radius (m)

T: Temperature (K)

Vm: Molecular volume of the solute at its boiling point = 0.034 and 0.025 m^3/Kmol for CO_2 and O_2, respectively.

V_T: Volume of the tank (m^3)

ν_A and ν_B: Diffusion volume coefficients of the solute and solvent ($\nu_{CO2} = 26.9$, $\nu_{O2} = 16.6$, $\nu_{H2O} = 10.73$).

ρ_L and ρ_g: Dynamic density of the liquid and gas, respectively (Kg/m^3)

σ: Surface tension of the solution

μ or μ_L: Viscosity of the solution (0.66 mNs/m^2 for cell culture medium is good approximation)

ORCID

0009-0002-3884-3217 (Naveenganesh Muralidharan)
0009-0006-9259-5284 (Thatsinee Johnson)
0009-0009-2162-6284 (Emma Bolduc)
0009-0000-3759-7486 (Mark Davis)

Conflicts of Interest

The authors declare no conflicts of interest.

Appendix

Appendix A1. *Algebraic mathematical simplification from Equation 30 to Equation 31.*

Step-1	$CTR_T. = KLa_{b,co2}.\left(\frac{\left(C_{l,co2}\left(1-Exp(-A_{co2})\right)+X_{b,in,Co2}.P_l.H_{Co2}.Exp(-A_{co2})-X_{b,in,co2}.P_l.H_{Co2}\right)}{A_{co2}}\right)$
Step-2	$CTR_T. = KLa_{b,co2}.\left(\frac{\left(C_{l,co2}\left(1-Exp(-A_{co2})\right)+X_{b,in,Co2}.P_l.H_{Co2}.(Exp(-A_{co2})-1)\right)}{A_{co2}}\right)$
Step-3	$CTR_T. = KLa_{b,co2}.\left(\frac{\left(C_{l,co2}\left(1-Exp(-A_{co2})\right)-X_{b,in,co2}.P_l.H_{Co2}.(1-Exp(-A_{co2}))\right)}{A_{co2}}\right)$
Step-4	$CTR_T = KLa_{b,co2}\left(\frac{\left(C_{l,co2}\left(1-Exp(-A_{co2})\right)-X_{b,in,co2}.P_l.H_{Co2}.(1-Exp(-A_{co2}))\right)}{A_{co2}}\right)$
Step-5	$CTR_T.A_{co2} = KLa_{b,co2}\left(\left(C_{l,co2}\left(1-Exp(-A_{co2})\right)-X_{b,in,co2}.P_l.H_{Co2}.(1-Exp(-A_{co2}))\right)\right)$
Step-6	$CTR_T.A_{co2} = \left(KLa_{b,co2}.C_{l,co2}\left(1-Exp(-A_{co2})\right)-\left(KLa_{b,co2}.X_{b,in,co2}.P_l.H_{Co2}.(1-Exp(-A_{co2}))\right)\right)$
Step-7	$CTR_T.A_{co2}+KLa_{b,co2}.X_{b,in,co2}.P_l.H_{Co2}.(1-Exp(-A_{co2})) = \left(KLa_{b,co2}.C_{l,co2}\left(1-Exp(-A_{co2})\right)\right)$
Step-8	$CTR_T.A_{co2}+KLa_{b,co2}.X_{b,in,co2}.P_l.H_{Co2}.(1-Exp(-A_{co2})) = KLa_{b,co2}.C_{l,co2}-KLa_{b,co2}.C_{l,co2}.Exp(-A_{co2})$
Step-9	$CTR_T.A_{co2}+KLa_{b,co2}.X_{b,in,co2}.P_l.H_{Co2}.(1-Exp(-A_{co2})) = C_{l,co2}(KLa_{b,co2}.-KLa_{b,co2}.Exp(-A_{co2})$
Step-10	$\frac{CTR_T.A_{co2}+KLa_{b,co2}.X_{b,in,co2}.P_l.H_{Co2}.(1-Exp(-A_{co2}))}{(KLa_{b,co2}.-KLa_{b,co2}.Exp(-A_{co2})} = C_{l,co2}$
Step-11	$C_{l,co2} = \frac{CTR_T.A_{co2}+KLa_{b,co2}.X_{b,in,co2}.P_l.H_{Co2}.(1-Exp(-A_{co2}))}{KLa_{b,co2}(1-Exp(-A_{co2})}$

References

[1] Hu, W. "SCALING UP AND SCALING DOWN ON CELL CULTURE BIOREACTORS." In Cell Culture Bioprocess Engineering, 2nd ed., 281. CRC Press, 2020.

[2] Muralidharan, N., Johnson, T., & Davis, M. (2023, November 16). Identifying False Metabolite Measurements During Cell-Culture Monitoring Effective Application of the Multivariate Hotelling's T2 Statistic. Bioprocess International, 21(11-12), 29-31. Retrieved from https://bioprocessintl.com/2023/november-december-2023/identifying-false-metabolite-measurements-during-cell-culture-monitoring-effective-application-of-the-multivariate-hotellings-t2-statistic/

[3] Xing, Z., Lewis, A. M., Borys, M. C., & Li, Z. J. (2017). A carbon dioxide stripping model for mammalian cell culture in manufacturing scale bioreactors. Biotechnology and Bioengineering, 114(6), 1184-1194. https://doi.org/10.1002/bit.26232

[4] DeZengotita, V. M., Schmelzer, A. E., & Miller, W. M. (2002). Characterization of hybridoma cell responses to elevated $pCO_2$and osmolality: Intracellular pH, cell size, apoptosis, and metabolism. Biotechnology and Bioengineering, 77(4), 369-380. https://doi.org/10.1002/bit.10176

[5] Mostafa, S. S., & Gu, X. (2003). Strategies for improved dCO_2 removal in large‐scale fed‐batch cultures. Biotechnology Progress, 19(1), 45-51. https://doi.org/10.1021/bp0256263

[6] Xing, Z., Kenty, B. M., Li, Z. J., & Lee, S. S. (2009). Scale‐up analysis for a CHO cell culture process in large‐scale bioreactors. Biotechnology and Bioengineering, 103(4), 733-746. https://doi.org/10.1002/bit.22287

[7] Hu, W. "OXYGEN TRANSFER IN CELL CULTURE BIOREACTORS." In Cell Culture Bioprocess Engineering, 2nd ed., 219. CRC Press, 2020.

[8] Wilke, C. R., & Chang, P. (1955). Correlation of diffusion coefficients in dilute solutions. AIChE Journal, 1(2), 264-270. https://doi.org/10.1002/aic.690010222

[9] Royce, P. N., & Thornhill, N. F. (1991). Estimation of dissolved carbon dioxide concentrations in aerobic fermentations. AIChE Journal, 37(11), 1680-1686. https://doi.org/10.1002/aic.690371111

[10] Muralidharan, N. (2023, February 9). Shear-Proof Design Space: Scaling Stirred-Tank Bioreactors for Cell Culture Processes. Bioprocess International, 21(1-2), 36-38. https://bioprocessintl.com/upstream-processing/bioreactors/shear-proof-design-space-scaling-stirred-tank-bioreactors-for-cell-culture-processes/

[11] Doran, P. M. (1995). Mass Transfer. In Bioprocess Engineering Principles (1st ed., p. 210- 213). Elsevier Science & Technology Books.

[12] Katoh, S., Horiuchi, J., & Yoshida, F. (2015). Mass Transfer. In Biochemical engineering: A textbook for engineers, chemists and biologists (2nd ed., p. 73- 77). John Wiley & Sons.

[13] Sieblist, C., Hägeholz, O., Aehle, M., Jenzsch, M., Pohlscheidt, M., & Lübbert, A. (2011). Insights into large‐scale cell‐culture reactors: II. gas‐phase mixing and CO_2 stripping. Biotechnology Journal, 6(12), 1547-1556. https://doi.org/10.1002/biot.201100153

[14] Liow, K. Y., Thouas, G. A., Tan, B. T., Thompson, M. C., & Hourigan, K. (2009). Modelling the transport of momentum and oxygen in an aerial-disk driven bioreactor used for animal tissue or cell culture. IFMBE Proceedings, 1672-1675. https://doi.org/10.1007/978-3-540-92841-6_415

[15] Stadler, E. L., & B. Braun Biotech Inc. (2001, October). Fermentor / Bioreactor Design Lecture [Paper presentation]. Bioprocess Equipment Design Seminar, Atlanta, GA.

[16] Fuller, E. N., Schettler, P. D., & Giddings, J. C. (1966). New method for prediction of binary gas-phase diffusion coefficients. Industrial & Engineering Chemistry, 58(5), 18-27. https://doi.org/10.1021/ie50677a007

[17] Muralidharan, N., Bolduc, E., & Davis, M. (2024, January/February). Characterizing Oxygen Mass Transfer and Shear During Cell Culture Calculating the Maximum Cell Density Supported By a 20,000-Liter Stirred-Tank Bioreactor. Bioprocess International, 22(1-2).

[18] Baz-Rodr'ıguez, S., Aguilar-Corona, A., & Soria, A. (2012). RISING VELOCITY FOR SINGLE BUBBLES IN PURE LIQUIDS. Revista Mexicana de Ingenier'ıa Qu'ımica, 11(2), 269-278. https://www.scielo.org.mx/pdf/rmiq/v11n2/v11n2a6.pdf

[19] Gramer, M. J., & Ogorzalek, T. (2007). A semi ‐ empirical mathematical model useful for describing the relationship between carbon dioxide, pH, lactate and base in a bicarbonate ‐ buffered cell ‐ culture process. Biotechnology and Applied Biochemistry, 47(4), 197-204. https://doi.org/10.1042/ba20070001

[20] Calderbank, P., & Moo-Young, M. (1961). The continuous phase heat and mass-transfer properties of dispersions. Chemical Engineering Science, 16(1-2), 39-54. https://doi.org/10.1016/0009-2509(61)87005-x